

THE UPPER PHOTOSPHERE AND LOWER CHROMOSPHERE OF SMALL-SCALE MAGNETIC FEATURES

S.K. SOLANKI, J.H.M.J. BRULS

Institute of Astronomy, ETH-Zentrum, CH-8092 Zürich, Switzerland

O. STEINER

Kiepenheuer Insitut für Sonnenphysik, Schöneckstr. 6, D-79104 Freiburg/Br, F.R.G.

T. AYRES

Center for Astrophysics and Space Astronomy, University of Colorado, Boulder, CO 80309-0391, USA

W. LIVINGSTON

National Solar Observatory, National Optical Astronomy Observatories, P.O. Box 26732, Tucson, AZ 85726, USA*

and

H. UITENBROEK

Harvard-Smithsonian Center for Astrophysics, 60 Garden Street, MA 02138, USA

Abstract. We empirically investigate the magnetic and thermodynamic properties of small-scale solar magnetic features in their upper photospheric and lower chromospheric layers. We find that the constraints set by the diagnostics we use (Mg I 12.32 μm line, Ca II K line, strong Fe lines, CO fundamental band lines, etc.) are well satisfied by the standard flux tube picture, if it is extended to include almost horizontal canopies in the lower chromosphere. These diagnostics also constrain the chromospheric temperature rise in flux tubes and their distribution and merging height. In addition, CO emission outside the solar limb is used to obtain information on the thermal structure of the chromosphere between the magnetic elements.

Key words: solar magnetism, solar activity, solar magnetic elements, magnetic flux tubes

1. Introduction

The thermodynamics of the quiet sun are well studied. For small-scale magnetic features, however, our knowledge of the magnetic and thermal structure has for a long time been restricted mainly to the lower and middle photosphere. Here we present some results of investigations constraining the thermal and magnetic structure of the upper photospheric and lower chromospheric layers in magnetic elements. We first discuss the thermal and magnetic structure of the upper photospheric layers of small-scale magnetic features and then move up to the lower chromosphere.

The basic model of magnetic elements underlying all the work presented here is the flux tube model. The magnetic features are assumed to be axially symmetric, with a sharp boundary. The field expands with height until it merges with neigh-

* Operated by the Association of Universities for Research in Astronomy, Inc. (AURA), under cooperative agreement with the National Science Foundation

bouring flux tubes. The main free parameters of the model are the field strength $B(z=0)$ and filling factor $\alpha(z=0)$ at the height of unit optical depth in the quiet sun ($z=0$), and the temperature stratifications inside and outside the magnetic features. Typical $B(z=0)$ values are 1400–1700 G (Rüedi et al. 1992) and $\alpha(z=0)$ ranges from a few percent in the quiet network to 20–30% in the strongest plage (for the types of observations considered here). Note that for a given temperature stratification $B(z=0)$ and $\alpha(z=0)$ determine B at all heights, as well as the shape of the flux tube. Line profiles in this model are generally calculated along typically 10–20 parallel rays and added together before comparison with the observations, which cannot spatially resolve the individual flux tubes.

2. Upper photosphere: Thermal structure

It is clear from filtergram observations (e.g. around the core of Ca II K, Mehlretter 1974) that the chromospheric temperature rise must begin at deeper geometrical layers within magnetic elements. The quantitative determination of the temperature stratification within magnetic features has, however, been in the past generally restricted to LTE or to unpolarized observations and calculations, so that the depth at which the chromospheric temperature rise begins could not be determined.

An NLTE investigation of the diagnostic properties of a number of Fe I and II spectral lines revealed that the shape of the Stokes V profile of Fe II 4923 Å (the strongest unblended Fe II line in the visible) is sensitive to the height at which the photospheric temperature rise within magnetic features begins. Figure 1 shows the temperature stratification of various flux tube models for which line profiles were calculated, as well as a quiet sun model for reference. The various flux-tube models differ mainly in the height at which the chromospheric temperature rise begins. In Fig. 2 we plot observed and calculated V profiles of Fe II 4923 Å for the various models and different macroturbulence ξ . Obviously, model PC2, with $\xi = 2 \text{ km s}^{-1}$ gives the best fit to the observed profile. The comparison of our model calculations with the observations thus suggests that in magnetic elements the chromospheric temperature rise begins 200–300 km deeper in the average quiet sun. Interestingly, there does not appear to be any significant difference between the magnetic elements in the network and those in active regions, although they differ significantly in their deeper layers.

Note that this diagnostic alone cannot distinguish clearly between the location and initial steepness of the temperature rise. A search for additional diagnostics would be useful to help settle the remaining uncertainties. For further details see Bruls and Solanki (1993).

3. Upper photosphere: magnetic structure

The prime diagnostic of upper photospheric magnetism are the 12 μm emission lines of Mg I, which, due to their large wavelength, are extremely Zeeman sensitive (e.g. Brault and Noyes 1983, Deming et al. 1988). The two main observational facts exhibited by these lines in solar plages are the relatively low field strength of 200–500 G (compared to 1500–2000 G seen in the 1.56 μm lines, which is formed at the

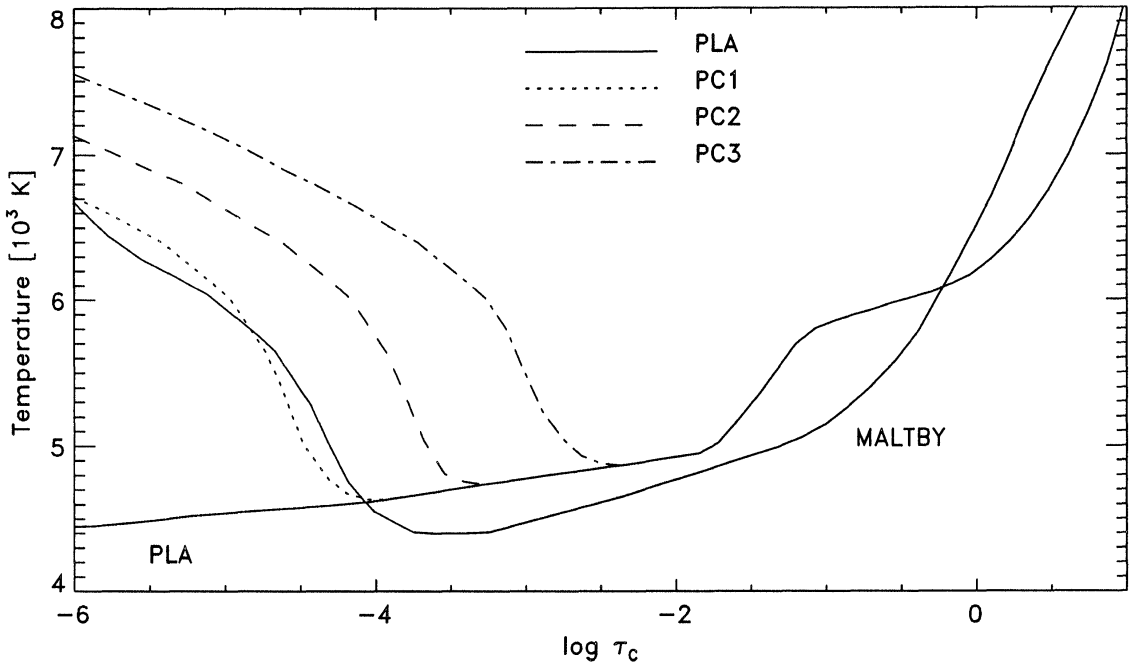


Fig. 1. Temperature vs. continuum optical depth τ_c at 5000 \AA for each plage flux-tube model. The model without a chromospheric temperature rise, marked PLA, reproduces the line profiles in LTE, the curve marked MALTBY represents the quiet sun model of Maltby et al. (1986).

bottom of the photosphere) and the wide variety of profile shapes seen in different plages (e.g. Zirin and Popp 1989).

We have synthesized the Mg I $12.32 \mu\text{m}$ line in flux tube models. We find that the profile shape and splitting of this line is not only sensitive to the field strength at the base of the flux tube $B(z=0)$, but also to the magnetic filling factor $\alpha(z=0)$ there. The sensitivity to α derives from the fact that for $\alpha \gtrsim 10\text{--}15\%$ this line is formed above the merging height of neighbouring flux tubes. The intrinsic field strength above the merging height is $\alpha(z=0) \times B(z=0)$, so that the splitting of this line [for large $\alpha(z=0)$] depends equally on $B(z=0)$ and $\alpha(z=0)$. This is in contrast to the spectral lines in the visible and near infrared, whose profile shape depends only on $B(z=0)$ and not on $\alpha(z=0)$. Fig. 3 shows the calculated profile for different $B(z=0)$ and $\alpha(z=0)$ values. It is evident from the figure that standard flux-tube models with reasonable parameters successfully reproduce the observed range of field strengths: The B_A values in the lower part of Fig. 3 represent the B determined from the splitting of the V profiles.

Another important property revealed by such calculations is that the shape of the line profile depends on the spatial distribution of the field, in the sense that the line profile is different if, e.g., the complete resolution element is filled by flux tubes at $\alpha(z=0) = 16\%$ or if flux tubes with $\alpha(z=0) = 32\%$ fill half the resolution element, while the other half is completely field free. This property, on the one hand, allows this line to give information on the subresolution distribution of magnetic flux, while, on the other hand, leading to a large variety of line shapes in active region plages,

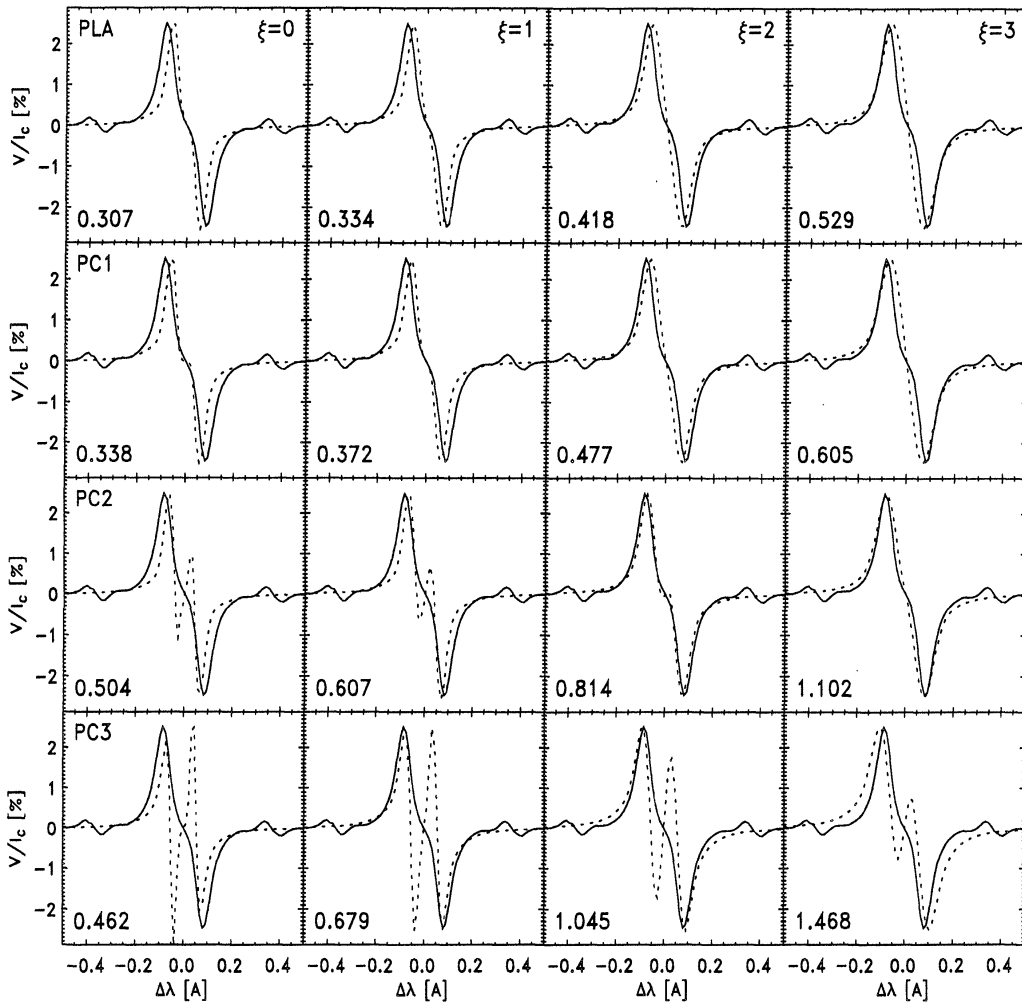


Fig. 2. Solid curves: Stokes V profile of Fe II 4923 Å observed in an active region plage. Dashed curves: Synthetic Stokes V profiles for the four plage models shown in Fig. 1 (rows; the models are specified in the leftmost column of each row), with different macro-turbulent smearing (columns; velocities are specified in the upper right corners in the top row).

in agreement with the observations of Zirin and Popp (1989). Additional details are given by Bruls and Solanki (1994).

4. Lower chromosphere: Thermal and magnetic structure

Before turning to small-scale magnetic features let us first consider the non-magnetic gas between them. The most intriguing question related to the thermal structure of the lower chromosphere concerns the existence and extent of cool clouds of gas (Ayres et al. 1986, Ayres 1991). According to past observations of molecular CO fundamental band spectra there appears to be a cool and dark component of the chromosphere having temperatures less than 4000 K, that coexists with the hot and bright gas of 6000–7000 K revealed by atomic lines. Because the CO data

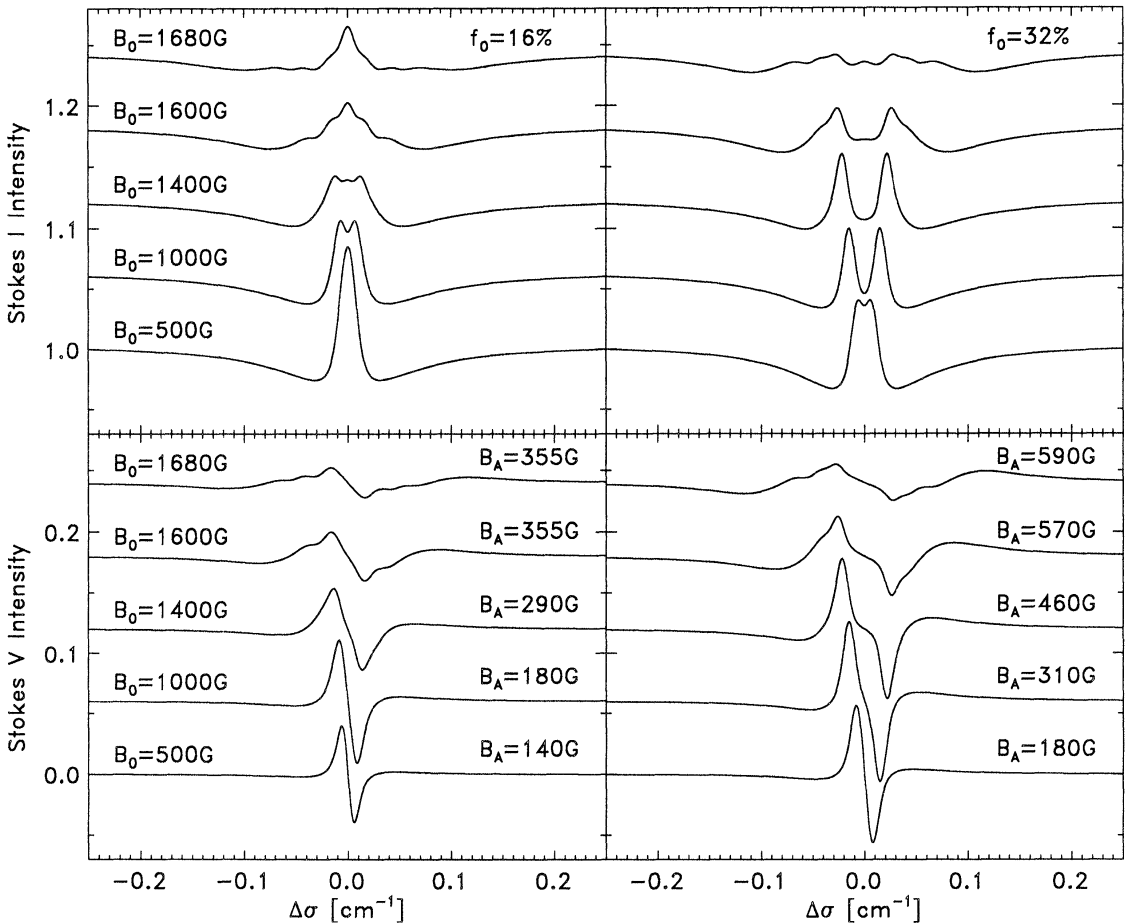


Fig. 3. Synthetic Mg I 12.32 μm Stokes I (top) and V profiles (bottom) for model PC2 with different $B_0 = B(z = 0)$. Filling factor $f_0 = \alpha(z = 0) = 16\%$ (left) and 32% (right). The profiles have been normalized and shifted vertically for clarity. In the lower panels the apparent magnetic field strength B_A corresponding to the splitting of the Stokes V peaks is indicated.

have previously been obtained with a modest resolution of several arc-sec, while the atomic information can be from sub-arc-sec flash spectra, the reality of the cool component is controversial. Controversy also surrounds the heights that CO spectral lines probe: is any dark component truly chromospheric, or are the lines simply responding to photospheric intergranular lanes? New CO spectra obtained at the diffraction limit of the McMath-Pierce telescope on Kitt Peak under conditions apparently devoid of seeing show that the 4.67 μm CO fundamental band lines go into emission beyond the limb just as do atomic species (Fig. 4, cf. Uitenbroek et al., these proceedings). This emission allows us to probe the chromosphere without the usual contamination from the photosphere. It shows that the cold gas seen in CO lines is definitely chromospheric. The observations can be explained most naturally by a cold chromospheric component, whose temperature drops as low as 3000–3500 K, which covers 50–85% of the quiet solar surface in the lower chromospheric layers and which is bounded at its upper end by a steep rise to normal chromospheric

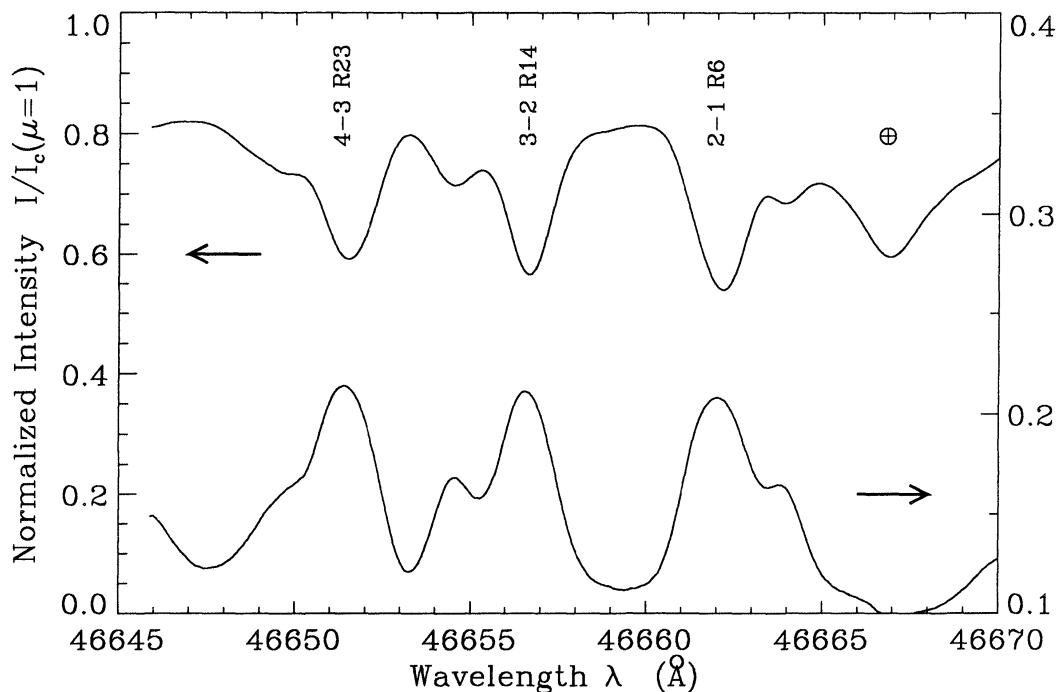


Fig. 4. Two spectra observed near the north pole while stepping the entrance slit across the solar limb. The upper spectrum lies inside the solar limb and exhibits absorption lines (it refers to the axis on the left), the lower spectrum lies outside the limb (and refers to the right axis). The three main CO features are identified; the line marked \oplus is produced in the earth's atmosphere. The off limb spectrum exhibits emission features at the same wavelength as the CO absorption lines on the disc.

temperatures of 6000–7000 K. This steep temperature rise takes place at a height of 900–1100 km.

A part of the hot material between these cool CO clouds lies within the magnetic elements (this is already suggested by the good correlation between chromospheric brightness indicators and the magnetic field). We consider here a simple model of the chromospheric thermal structure, which assumes that *all* the hot material lies within the magnetic features, which are surrounded by the cool CO clouds. In such a model the magnetic structure of the flux tubes, calculated to satisfy complete force balance, flares out extremely rapidly at a certain height in the lower or middle chromosphere, thus forming a magnetic canopy. The base height of this canopy depends mainly on the thermal stratification within and outside the flux tubes. For a hot flux tube in cool surroundings the internal pressure scale height is large while the external scale height is small. Even if the internal pressure is smaller than the external pressure in the photosphere (as required by horizontal pressure balance), the difference in pressure scale heights means that at a certain critical height the internal pressure equals the external pressure. A horizontal canopy is formed at this height, since the external gas cannot confine the field above this height. The larger the temperature contrast, the lower the canopy base.

The base height of the canopy can also be deduced accurately by calculating Ca II K profiles in the flux tube model and comparing them with observations under the assumption that the magnetic and thermal canopy bases are identical. The strength of the K₂ peaks and its spatial variation turns out to be extremely sensitive to the height of the thermal canopy base. The canopy base height is found to lie between 900 and 1100 km, in agreement with canopy base heights deduced from observations (Giovanelli and Jones 1982, Faurobert-Scholl 1992, 1994). The thermal canopy base derived from the Ca II K line agrees very well with that derived from the emission lines of CO at the limb, so that the assumption that the magnetic and thermal canopy are identical is at least self-consistent. The above applies mainly to the quiet sun. In active regions flux tubes often merge below the height of the classical temperature minimum.

A detailed description of this work is given by Solanki and Steiner (1990) and Solanki et al. (1991, 1994).

5. Conclusions

The main conclusion we reach is that the standard flux tube model of small-scale magnetic features passes a number of stringent tests imposed by observations of the lower chromosphere and the upper photosphere. A picture of the thermal and magnetic structure of magnetic elements is emerging which can satisfy a large number of observational constraints. In this picture the chromospheric temperature rise begins 200–300 km deeper within magnetic elements than in a model of the average quiet chromosphere. On the other hand, over much of the remaining surface of the quiet sun a hot chromosphere only starts at a height of 900–1100 km, with very cool gas (3000–3500 K) underlying large parts of this thermal canopy. The flux tube magnetic field expands very rapidly in the quiet chromosphere and forms an almost horizontal magnetic canopy at roughly the same height as the thermal canopy.

In active regions neighbouring flux tubes merge at or below the temperature minimum, so that little cold gas is present and no horizontal canopies are formed. 12 μm observations suggest that the merging height varies rapidly across an active region. The wide variety of profile shapes of this line observed in active region plages, like the variation of the merging height, comes from the very inhomogeneous spatial distribution of flux tubes.

References

- Ayres T.R., 1991, in *Mechanisms of Chromospheric and Coronal Heating*, R. Ulmschneider, E.R. Priest, R. Rosner (Eds.), Springer, Heidelberg, p. 228
 Ayres T.R., Testerman L., Brault J.W., 1986, *Astrophys. J.* **304**, 542
 Brault J.W., Noyes R.W., 1983, *Astrophys. J.* **269**, L61
 Bruls J.H.M.J., Solanki S.K., 1993, *Astron. Astrophys.* **273**, 293
 Bruls J.H.M.J., Solanki S.K., 1994, *Astron. Astrophys.* in press
 Deming D., Boyle R.J., Jennings D.E., Wiedemann G., 1988, *Astrophys. J.* **333**, 978
 Faurobert-Scholl M., 1992, *Astron. Astrophys.* **258**, 521
 Faurobert-Scholl M., 1994, *Astron. Astrophys.* in press
 Giovanelli R.G., Jones H.P., 1982, *Solar Phys.* **79**, 267
 Maltby P., Avrett E.H., Carlsson M., Kjeldseth-Moe O., Kurucz R.L., Loeser R., 1986, *Astrophys. J.* **306**, 284

- Mehlretter J.P., 1974, *Solar Phys.* **38**, 43
Rüedi I., Solanki S.K., Livingston W., Stenflo, J.O., 1992, *Astron. Astrophys.* **263**, 323
Solanki S.K., Steiner O., 1990, *Astron. Astrophys.* **234**, 519
Solanki S.K., Steiner O., Uitenbroek H., 1991, *Astron. Astrophys.* **250**, 220
Solanki S.K., Livingston W., Ayres T., 1994, *Science* **263**, 64
Zirin H., Popp B., 1989, *Astrophys. J.* **340**, 571